Novel metric for analysis, interpretation and visualization of BRDF data

MIKHAIL LANGOVOY and GERD WUEBBELER and CLEMENS ELSTER, Physikalisch-Technische Bundesanstalt

Characterizing the appearance of real-world surfaces is a fundamental problem in multidimensional reflectometry, computer vision and computer graphics. For many applications, appearance is sufficiently well characterized by the bidirectional reflectance distribution function (BRDF). The BRDF is one of the fundamental concepts in such diverse fields as computer graphics, computer vision and reflectometry. We construct a new class of measures of quality of fit for BRDF models. The proposed distance is constructed to reflect basic characteristics of human perception and leads to physically meaningful conclusions for BRDF data analysis.

We prove the boundedness of new quasi-distances, and show that they induce an absolute scale of distances on the space of BRDFs. Our bounds are stronger than the inequalities obtained by standard methods, and therefore we provide better approximations of induced absolute scales of distances on the space of BRDFs. We discuss common points and differences between BRDF analysis in computer graphics and computer vision on one hand, and in metrology and reflectometry on the other hand.

Categories and Subject Descriptors: I.2.10 [**Artificial Intelligence**]: Vision and Scene Understanding—*Perceptual reasoning, Modeling and recovery of physical attributes*; I.3.6 [**Computer Graphics**] Methodology and techniques; I.3.5 [**Computer Graphics**] Physically based modeling; G.3 [**Probability and Statistics**] Nonparametric statistics, Multivariate statistics; I.6.4 [**Simulation and Modeling**] Model Validation and Analysis

General Terms: Theory, Measurement, Human Factors

Additional Key Words and Phrases: BRDF, diffuse reflection, specular reflection, computer graphics, computer vision, metrology, data analysis, statistics of manifolds, distance on the space of BRDFs

1. INTRODUCTION

Characterizing the appearance of real-world surfaces is a fundamental problem in multidimensional reflectometry, computer vision and computer graphics. For many applications, appearance is sufficiently well characterized by the bidirectional reflectance distribution function (BRDF).

In the case of a fixed wavelength, the BRDF describes reflected light as a four-parameter function of incoming and outgoing light directions. In the special case of rotational symmetry, isotropic BRDFs are used. Isotropic BRDFs are functions of only three angles. The BRDF is applied under the assumption that all light falls at a single surface point. The classical device for measuring BRDFs is the gonio-reflectometer

This work has been carried out within EMRP project IND 52 'Multidimensional reflectometry for industry'. The EMRP is jointly funded by the EMRP participating countries within EURAMET and the European Union. The authors thank Monika Walzel for her technical assistance in preparing the manuscript.

Permission to make digital or hard copies of part or all of this work for personal or classroom use is granted without fee provided that copies are not made or distributed for profit or commercial advantage and that copies show this notice on the first page or initial screen of a display along with the full citation. Copyrights for components of this work owned by others than ACM must be honored. Abstracting with credit is permitted. To copy otherwise, to republish, to post on servers, to redistribute to lists, or to use any component of this work in other works requires prior specific permission and/or a fee. Permissions may be requested from Publications Dept., ACM, Inc., 2 Penn Plaza, Suite 701, New York, NY 10121-0701 USA, fax +1 (212) 869-0481, or permissions@acm.org.
© YY ACM 1544-3558/YY/01-ART $15.00
DOI 10.1145/0000000.0000000 http://doi.acm.org/10.1145/0000000.0000000

Höpe and Hauer [2010], which is composed of a photometer and light source that are moved relative to a surface sample under computer control.

In computer graphics and computer vision, usually either physically inspired analytic reflectance models [Oren and Nayar 1995], [Cook and Torrance 1981], [He et al. 1991], or parametric reflectance models chosen via qualitative criteria [Lambert and Anding 1892], [Phong 1975], [Blinn 1977], [Lafortune et al. 1997] are used to model BRDFs. These BRDF models are only crude approximations of the reflectance of real materials. Moreover, analytic reflectance models are limited to describing only special subclasses of materials.

In multidimensional reflectometry, an alternative approach is usually taken. One measures values of the BRDF directly for different combinations of the incoming and outgoing angles and then fits the measured data to a selected analytic model using optimization techniques. There are several shortcomings to this approach as well.

A possible alternative to parametric models is in using properly designed simulation studies together with modern data-driven nonparametric estimates of multidimensional manifolds to construct more realistic BRDFs. As an example of this approach, [Matusik 2003] and [Matusik et al. 2003] modelled the reflectance of materials in nature as a linear combination of a small set of basis functions derived from analyzing a large number of densely sampled BRDFs of different materials.

In computer graphics, it is important that BRDF models should be processed in real-time. Computer-modeled materials have to remind real materials qualitatively, but quantitative accuracy is not as important. The picture in reflectometry and metrology is almost the opposite: there is typically no need in real-time processing of BRDFs, but quantitative accuracy is paramount. In view of this, some of the breakthrough results from computer vision and animation would not fit applications in reflectometry and also in industry.

Another difference to virtual reality models is that in computer graphics measurement errors are essentially never considered. This is not the case in metrology, reflectometry and in any real-world based industry [Höpe et al. 2014]. Since measurement errors can greatly influence shape and properties of BRDF manifolds, there is a clear need to develop new methods for handling BRDFs in the presence of measurement errors.

In this paper, we treat BRDF measurements as samples of points from a high-dimensional and highly non-linear non-convex manifold. We argue that any adequate statistical analysis of BRDF measurements has to account both for the nonlinear structure of the data as well as for an ill-behaved noise. Standard statistical methods for the analysis of errors can not be safely applied to BRDF data.

In computer science literature on BRDFs, there are few papers that study the quality of fit of BRDF models to real data, see [Ngan et al. 2005], [Shirley et al. 1997]. Even fewer studies attempt to do a more rigorous statistical analysis, either for the quality of fit or for the influence of errors. Most of these studies use the (most standard) L_2-norm, see [Arvo et al. 1994], [Rushmeier et al. 1995]. As we show in Section 6 of this paper, L_p-norms do not adequately reflect some core characteristics of human perception.

In this paper we propose and construct a new class of measures of quality of fit for BRDF models. We will use these measures to evaluate the influence of measurement and model errors on both real and simulated BRDFs. Our measure of distance between BRDFs is constructed to reflect basic characteristics of human perception. The new measure is leading to physically meaningful conclusions at least for some basic applications of BRDF data analysis. This is a necessary property as our analysis has to be applicable to physical objects and real data and has to make sense in terms of human perception.

2. MAIN DEFINITION

The BRDF, $f_r(\omega_i, \omega_r)$ is a four-parameter function that defines how light is reflected at an opaque surface. The function takes an incoming light direction, ω_i, and outgoing direction, ω_r, both defined with respect to the surface normal $\mathbf{n}$, and returns the ratio of reflected radiance exiting along ω_r to the irradiance incident on the surface from direction ω_i. Each direction ω is itself parameterized by the azimuth angle ϕ and the Zenith

angle θ, therefore the BRDF as a whole is four-dimensional. The BRDF has units sr^{-1}, with steradians (sr) being a unit of solid angle.

The BRDF was first defined by Nicodemus in [Nicodemus 1965]. According to [Nicodemus 1965],

$$f_r(\omega_i, \omega_r) = \frac{\mathrm{d}\, L_r(\omega_r)}{\mathrm{d}\, E_i(\omega_i)} = \frac{\mathrm{d}\, L_r(\omega_r)}{L_i(\omega_i) \cos\theta_i \, \mathrm{d}\, \omega_i}, \tag{1}$$

where L is radiance, or power per unit solid-angle-in-the-direction-of-a-ray per unit projected-area-perpendicular-to-the-ray, E is irradiance, or power per unit surface area, and θ_i is the angle between ω_i and the surface normal, $\mathbf{n}$. The index i indicates incident light, whereas the index r indicates reflected light.

3. IMPORTANT MODELS

3.1 Diffuse reflection

The Lambertian model [Lambert and Anding 1892] represents reflection of perfectly diffuse surfaces by a constant BRDF. Because of its simplicity, the Lambertian model is extensively used as one of the building blocks for models in computer graphics. It was believed for a long time that the so-called standard diffuse reflection materials exhibit Lambertian reflectance, but recent studies with actual BRDF measurements convincingly reject this hypothesis [Höpe and Hauer 2010].

The Oren-Nayar model [Oren and Nayar 1995] is a "directed–diffuse" microfacet model, with perfectly diffuse (rather than specular) microfacets. It can be viewed as a generalization of the Lambertian model. This is a reflectance model for diffuse reflection from rough surfaces. The Oren-Nayar model is typically used to predict the appearance of rough surfaces, such as concrete or sand.

Resently, a more sophisticated model was proposed in [Simonot 2009]. This new model includes as special cases both the Lambertian model and the Oren–Nayar model, as well as the Torrance–Sparrow model with specular microfacets.

The Lommel-Seeliger model [Fairbairn 2005] is used to simulate the brightening of a rough surface when illuminated from directly behind the observer. This is a physically inspired model of a special class of reflections from diffuse surfaces. This model is typically applied to model astronomical data, such as lunar and Martian reflection.

3.2 Specular reflection and combined models

The Phong reflectance model [Phong 1975] is a phenomenological model intended to represent plastic-like specularity. This reflection model describes the way a surface reflects light as a combination of the diffuse reflection of rough surfaces with the specular reflection of shiny surfaces. It is based on an idea that shiny surfaces have small intense specular highlights, while dull surfaces have large highlights that fall off more gradually. The model has been extensively used in computer graphics, but nowadays it is considered too crude and is replaced by newer approaches. For applications in reflectometry and metrology, this model does not seem to lead to a good fit to real materials.

The Blinn-Phong model reduces the computational overhead of the Phong model via allowing for certain quantities to be interpolated [Blinn 1977]. There is a computational advantage over the Phong model, but the quality of fit is not improved.

The Torrance-Sparrow model is a general model representing surfaces as distributions of perfectly specular microfacets [Torrance and Sparrow 1967].

The Cook-Torrance model [Cook and Torrance 1981] is a further advancement of the specular–microfacet Torrance-Sparrow model, accounting for wavelength and thus color shifting.

The He–Torrance–Sillion–Greenberg model [He et al. 1991] is physically based. This model attempts to take into account a variety of possible physical phenomena such as polarization, diffraction, interference, conductivity, grazing rays.

The Lafortune model [Lafortune et al. 1997] is a generalization of the Phong model with multiple possible specular lobes.

The Lebedev model is designed for analytical–grid BRDF approximation.

The Ward model [Ward 1992] is a specular–microfacet model with an elliptical-Gaussian distribution function dependent on surface tangent orientation (in addition to surface normal). It is an approximate model that does not reproduce the Fresnel effect.

The Ashikhmin–Shirley model [Ashikhmin and Shirley 2000] allows for anisotropic reflectance, along with a diffuse substrate under a specular surface. A related model is developed in [Ashikhmin and Premoze 2007]. These models use, in particular, the microfacets idea combined with the Phong reflectance model. Both models are computationally intensive, but are known to give good approximation to BRDFs of some real materials.

4. BASIC PROPERTIES OF DISTRIBUTIONS IN BRDF DATA

In our choice of data analysis procedures for BRDF models, we have to take into account specific properties of BRDF data. It is important to notice that, due to the complicated structure of measurement devices, outliers are possible in the data. Additionally, due to technical difficulties in measuring peak values of BRDFs (see [Ouarets et al. 2013], [Obein et al. 2014]), we have to account for the fact that certain (even though small) parts of the data contain observations with large errors. This also leads us to the conclusion that, even for simplest additive error models, we cannot blindly assume that random errors are identically distributed throughout the whole manifold. Additionally, missing data are possible and even inevitable for certain angles. Measurement angles themselves can be also arbitrary and non-uniformly distributed.

In view of the above arguments, a useful data analysis procedure for any BRDF model has to exhibit certain robustness against outliers and dependent or mixed errors.

A statistical procedure has to be universal enough in the sense that it has to be applicable to BRDF samples without requiring extra regularity in the data set, such as uniformly distributed (or other pre-specified) design points, pre-specified large number of measurements, or absence of missing values. This observation suggests that simple and robust methods are more practical for BRDF data than complicated (even if possibly asymptotically optimal) methods, as the latter class of procedures has to rely on rather strict regularity assumptions about the underlying model.

BRDF measurements represent a sample of points from a high-dimensional and highly non-linear non-convex manifold. Moreover, these measurements are collected via a nontrivial process, possibly involving random or systematic measurement errors of digital or geometric nature. These two observations suggest that any realistic statistical analysis of BRDF measurements has to account both for the nonlinear structure of the data as well as for a very ill-behaved noise. Standard statistical methods typically assume nice situations like i.i.d. normal errors, and can not be safely directly applied to BRDF data. Our study of statistical estimation for BRDF models in [Langovoy et al. 2014] clarified certain pitfalls in the analysis of BRDF data, and helped to understand and develop more refined estimates for more realistic BRDF models.

5. STATISTICAL ANALYSIS OF BRDF MODELS

Suppose we have measurements of a BRDF available for the *set of incoming angles*

$$\Omega_{inc} = \left\{\omega_i^{(p)}\right\}_{p=1}^{P_{inc}} = \left\{\left(\theta_i^{(p)}, \varphi_i^{(p)}\right)\right\}_{p=1}^{P_{inc}}. \tag{2}$$

Here $P_{inc} \geq 1$ is the total number of incoming angles where the measurements were taken. Say that for an incoming angle $\{\omega_i^{(p)}\}$ we have measurements available for angles from the *set of reflection angles*

$$\Omega_{refl} \;=\; \bigcup_{p=1}^{P_{inc}} \Omega_{refl}(p)\,, \tag{3}$$

where

$$\Omega_{refl}(p) \;=\left\{\omega_r^{(q)}\right\}_{q=1}^{P_{refl}(p)} =\left\{\left(\theta_r^{(q)},\varphi_r^{(q)}\right)\right\}_{q=1}^{P_{refl}(p)}, \tag{4}$$

where $\left\{P_{refl}(p)\right\}_{p=1}^{P_{inc}}$ are (possibly different) numbers of measurements taken for corresponding incoming angles.

Overall, we have the set of random observations

$$\left\{f\left(\theta_i^{(p)},\varphi_i^{(p)},\theta_r^{(q)},\varphi_r^{(q)}\right)\,\middle|\,\left(\theta_i^{(p)},\varphi_i^{(p)}\right)\in\Omega_{inc}\,,\,\left(\theta_r^{(q)},\varphi_r^{(q)}\right)\in\Omega_{refl}(p)\right\}. \tag{5}$$

Our aim is to infer properties of the BRDF funtion (1) from the set of observations (5). In general, the connection between the true BRDF and its measurements is described via a stochastic transformation T, i.e.

$$f(\omega_i,\,\omega_r) \;=\; T\big(f_{\text{true}}(\omega_i,\,\omega_r)\big)\,, \tag{6}$$

where f_{true} is the true BRDF and

$$T\;:\;\mathcal{M}\times\mathcal{P}\times\mathcal{F}_4\;\to\;F_4\,, \tag{7}$$

with $\mathcal{M} = (M,\mathfrak{A},\mu)$ is an (unknown) measurable space, $\mathcal{P} = (\Pi,\mathfrak{P},\mathbb{P})$ is an unknown probability space, $\mathcal{F}_4$ is the space of all Helmholtz-invariant energy preserving 4-dimensional BRDFs (see Definition 1 below), and F_4 is the set of all functions of 4 arguments on the 3-dimensional unit sphere S^3 in $\mathbb{R}^4$.

Equations (6) and (7) mean that there could be errors of both stochastic or non-stochastic origin. In this setting, the problem of inferring the BRDF can be seen as a statistical inverse problem. However, contrary to much literature on this subject, we do not assume linearity of the transformation T, we do not assume that T is purely stochastic, and we do not assume an additive model with zero-mean parametric errors, as these assumptions do not seem realistic for BRDF measurements. Of course, this setup is intractable in full generality, but for special cases we would be able to obtain quite general solutions.

6. FOUNDATIONS OF SENSITIVITY ANALYSIS FOR BRDF MODELS

In order to evaluate the influence of measurement errors and to be able to measure the quality of fit of BRDF models, we need a "measure of distance" between BRDFs. This measure must be reasonable from a qualitative viewpoint and it has to be physically reasonable, instead of merely providing us with a number for a pair of BRDFs.

There are many measures of distance and quasi-distance used in mathematics and statistics: L_p, $1 \leq p < +\infty$, L_∞, Sobolev distances [Sobolev Sobolev], Kullback-Leibler information divergence [Kullback and Leibler 1951], Mahalanobis [Mahalanobis 1936] and Minimum Description Length distances, chi-squared distance used in correspondence analysis [Langovaya et al. 2013], and other types of metrics and pseudo-metrics. Not all of them are appropriate for applications related to BRDFs.

In computer science literature on BRDFs, there are few papers that study the quality of fit of BRDF models to real data. Even fewer studies attempt to do a more rigorous statistical analysis, either for quality of fit or for influence of errors. Most of these studies use the (most standard) L_2-norm. Namely, for BRDFs $f_1 = f_1(\omega_i, \omega_r)$, $f_2 = f_2(\omega_i, \omega_r)$

$$L_2^2(f_1, f_2) = \int\int\int\int_{\Omega} \left\|(f_1 - f_2)(\theta_i, \phi_i, \theta_r, \phi_r)\right\|^2 d\theta_i \, d\phi_i \, d\theta_r \, d\phi_r \,, \tag{8}$$

where Ω is the set containing all possible values of the four parameters, in this case,

$$\Omega = \Theta_i \times \Phi_i \times \Theta_r \times \Phi_r \,. \tag{9}$$

Notice that Ω can be different for other BRDFs or in those cases where other restrictions are imposed.

It is known from both mathematics and statistics that not all distances are equally appropriate in all applications. More specifically, for a problem related to a functional class $\mathcal{F}$, only those distances are potentially applicable that are either defined or could be extended for all functions from $\mathcal{F}$.

As an example, for problems dealing with extremely heavy-tailed distributions with infinite variance, both the L_2-distance as well as related least squares methods, are not applicable. This example explains why we should not blindly use L_2-metrics for the analysis of BRDF data. Instead, we develop an appropriate "metric" for BRDFs.

Definition 1. *Let $\mathcal{F}_4$ be the* space of all Helmholtz-invariant energy preserving 4-dimensional BRDFs*. More precisely,*

$$\begin{aligned} \mathcal{F}_4 = \{ & f : \Theta_i \times \Phi_i \times \Theta_r \times \Phi_r \to \mathbb{R}_+ \quad \textit{such that} \\ & f(\theta_i, \phi_i, \theta_r, \phi_r) = f(\theta_r, \phi_r, \theta_i, \phi_i) \quad \textit{for all} \quad \theta_i, \phi_i, \theta_r, \phi_r \quad \textit{and} \\ & \int_{\Theta_r \times \Phi_r} f(\theta_r, \phi_r, \theta_i, \phi_i) \cos\theta_r \, d\theta_r \, d\phi_r \leq 1 \quad \textit{for all} \quad \theta_i, \phi_i \} \,. \end{aligned} \tag{10}$$

Any good metric for BRDFs shall not only be defined over $\mathcal{F}_4$, but this metric also should be leading to meaningful conclusions in terms of both physics and human perception.

Notice that the energy conservation inequality from (10) does not even imply

$$\int_{\Omega} \left\|f\right\|^2 d\mu_{\Omega} < +\infty \,,$$

where μ_{Ω} is a product measure on Ω. Therefore, $\mathcal{F}_4$ contains functions with extremely heavy tails.

There are two main directions for further developments.

Direction 1. Perform studies and do virtual experiments for the case when heavy-tailed distributions are used to model specular peaks.

Pros: 1. Virtual experiments with heavy-tailed distributions are of much interest on their own. Moreover, they help to locate the borderline between "nice and smooth" models and their parameter range, and extreme cases where most of the standard data analysis methods are not applicable. This is an important part of analysis of sensitivity.

2. Approximations are avoided. In particular, if BRDFs with peaks are precisely measured (see planned experiments in [Ouarets et al. 2013], [Obein et al. 2014]), all of the information will be utilized.

Cons. Surprisingly, currently there is no method to generate random variables with extremely heavy-tailed distributions with high accuracy! This is a big obstacle for applications in metrology where a high precision

is needed. A paper [Langovoy and Shneer 2014] is aiming to solve this problem by providing an algorithm for generating extreme heavy tails with perfect fit.

Direction 2. Smooth out outliers, gross errors and heavy-tailed peaks, but in a mathematically and physically reasonable way.

Pros: 1. Modeling and data analysis become methodologically easier.

2. As extremely high values of BRDFs at specular peaks are not measured with adequate precision, no grossly inaccurate or badly corrupted measurement with high value could enter the analysis and comparisons.

Cons. A choice of metric of distance between BRDFs is important, as smoothing out the extremes has to give a result that is physically sensible. However, a physically sensible metric opens advantageous opportunities.

Direction 1 will be our future direction of research, especially after high precision peak measurements will be available. Under the present conditions, it makes the most sense to follow Direction 2. Now let us focus once again on a proper metric for $\mathcal{F}_4$.

We start with a series of motivating examples. Notice that the majority of materials (and even some diffuse reflection standards) have a specular component, at least for a range of $\theta_i^{spec} \leq \theta < \pi/2$, for some incoming angle $\theta_i^{spec} > 0$. The specular component is responsible for shiny areas on the surface of the illuminated object. They are very distinct for the human observer.

Our main idea can be formulated as follows:

$$\left(\textit{ a "distance" } d \textit{ between BRDFs is physically reasonable } \right) \text{ if and only if } \left[\left\{ \; d(f_1, f_2) \textit{ is small } \right\} \text{ if and only if } \left\{ \textit{ two balls illuminated according to } f_1 \textit{ and } f_2 \textit{ would look similar to a human observer } \right\} \right].$$

To be more precise: in the above statement, we consider two balls of the same size that are made of materials with BRDFs f_1 and f_2 respectively. Both balls are illuminated with a point source of light. Notice that, in general, both the type of the light source as well as the shape of the illuminated object are important for human perception [Fleming et al. 2003].

Example 1. Suppose we are dealing with a point source of light, and fix the incoming light angles θ_i, ϕ_i. In the example on Figure 1, the upper half shows the cross sections of two different BRDFs, while the circles below each of the BRDFs are illustrating the resulting visual appearance of the balls that were made from materials with these BRDFs. These illuminated balls look very similar to a human observer. Meanwhile, an L_p-distance between f_1 and f_2 is large. From Example 1 we conclude that the position of the BRDF's peak is more important for a human observer than the peak's height and shape.

Example 2. Here an L_p-distance can be made small, since a very thin second peak of f_2 gives a small contribution to the integral. However, the difference between f_1 and f_2 is substantial for a human observer, as the second shiny place on the right ball is clearly noticeable. From Example 2 we conclude that the number of BRDF's peaks is important. Missing any peaks or adding unnecessary peaks is noticeable, so a good distance on $\mathcal{F}_4$ should penalize for missing or added peaks.

Example 3. For the same fixed θ_i, ϕ_i, see Figure 3. From Example 3 we conclude that locations of peaks are also important for an observer. This point is addressed by L_p-distances as well, though.

We focused on peaks in our examples, because L_p- and L_∞-metrics are dominated by peaks.

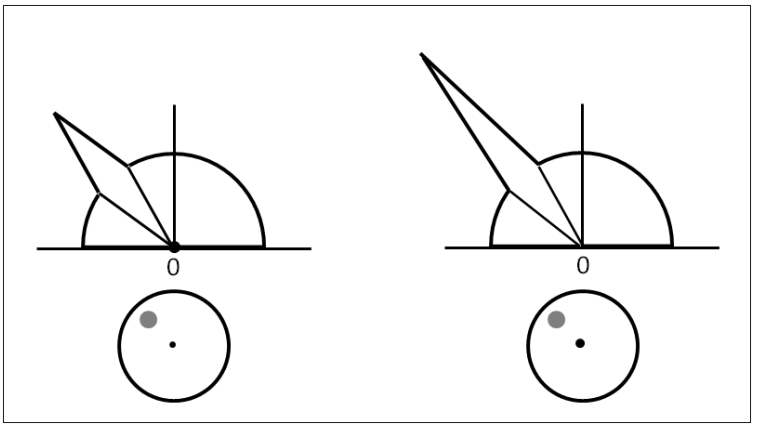

Fig. 1: Large L_p-distance, small difference in appearance

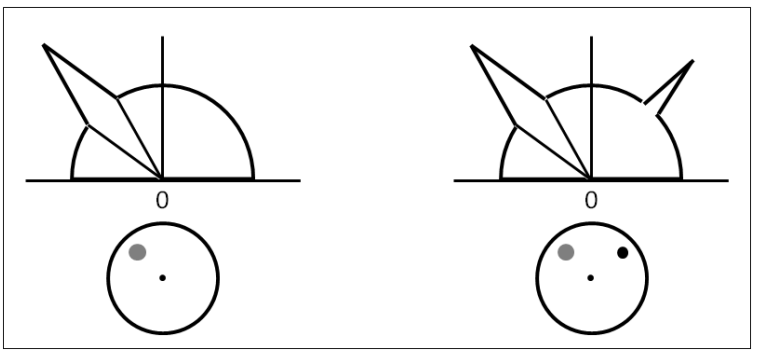

Fig. 2: Small L_p-distance, but visible difference in appearance

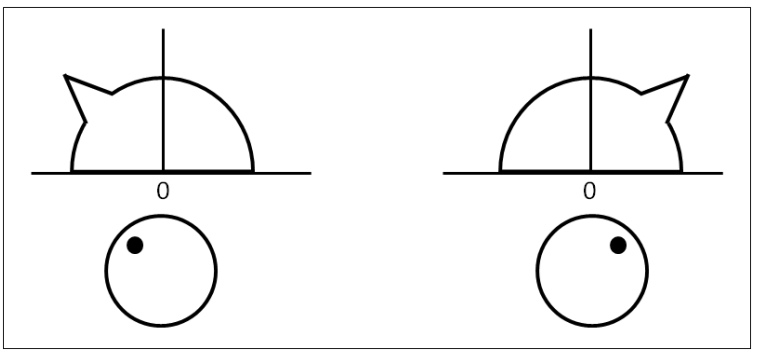

Fig. 3: Locations of peaks are important

7. MEASURE OF DISTANCE BETWEEN BRDFS

The following reasonable decomposition is typically used in BRDF studies:

$$BRDF(\theta_i, \varphi_i, \theta_r, \varphi_r) \,=\, f_{diff}(\theta_i, \varphi_i, \theta_r, \varphi_r) \,+\, f_{spec}(\theta_i, \varphi_i, \theta_r, \varphi_r)\,. \tag{11}$$

The above decomposition is given pointwise and in spherical coordinates. It is assumed that all BRDFs and their decompositions are μ_Ω-measurable functions. We assume that either for all $(\theta_i, \varphi_i, \theta_r, \varphi_r) \in \Omega$

$$f_{diff}(\theta_i, \varphi_i, \theta_r, \varphi_r) \,\cdot\, f_{spec}(\theta_i, \varphi_i, \theta_r, \varphi_r) \,=\, 0\,, \tag{12}$$

or, almost equivalently, that

$$\int_\Omega \big| f_{diff} \,\cdot\, f_{spec} \big| (\theta_i, \varphi_i, \theta_r, \varphi_r)\, d\mu_\Omega \,=\, 0\,. \tag{13}$$

Therefore, for each BRDF $f \in \mathcal{F}_4$ we have a decomposition of the parameter space Ω

$$\Omega \,=\, \Omega_{diff}(f) \cup \Omega_{spec}(f)\,, \quad \mu_\Omega\big(\Omega_{diff}(f) \cap \Omega_{spec}(f)\big) \,=\, 0\,. \tag{14}$$

As before, we denote $\omega_i \,=\, (\theta_i, \varphi_i)$, $\omega_r \,=\, (\theta_r, \varphi_r)$, $\omega \,=\, (\omega_i, \omega_r)$. Our goal is to construct μ_{BRDF}, a "metric" on the BRDF-space $\mathcal{F}_4$. Then the following decomposition is possible:

$$\mu_{BRDF}(f) \,=\, \mu_{diff}(f) \,+\, \mu_{spec}(f) \tag{15}$$

where we denote $\mu_{BRDF}(f) \,=\, \mu_{BRDF}(f, 0)$, a distance between f and 0 (i.e., an absolutely light-absorbing surface). Decomposition (15) holds if we put, say,

$$\mu_{diff}(f) \,=\, \mu_{BRDF}(f)\Big|_{\Omega_{diff}(f)}, \quad \mu_{spec}(f) \,=\, \mu_{BRDF}(f)\Big|_{\Omega_{spec}(f)}\,. \tag{16}$$

An important point is that μ_{diff} and μ_{spec} could and should be different.

Notice that our definition of Ω_{spec} and Ω_{diff} are formal and technical, and they do not have to correspond exactly to the physical phenomena of specular or diffuse reflection. Our definition allows us to split the area of glossy reflection between Ω_{spec} and Ω_{diff} without having to treat glossy reflection separately. In this paper we use the following rule to define a "specular" and a "diffuse" part of the BRDF.

Definition 2.

$$\Omega_{spec}(f) \,=\, \{\omega \,|\, f(\omega) \,\geq\, \Delta_1\} \tag{17}$$

$$\Omega_{diff}(f) \,=\, \Omega \setminus \Omega_{spec}(f) \tag{18}$$

For a data-driven automated choice of Δ_1, it is also possible to use spatial scan estimators introduced in [Langovoy et al. 2011a] and [Langovoy et al. 2011b].

Definition 3. *Let f_1, f_2 be BRDFs. Define the* element of distance *between f_1 and f_2 in $\mathcal{F}_4$ at a point ω as*

$$\rho_{BRDF}(f_1,f_2)(\omega) = \begin{cases} \rho_{diff}(f_1(\omega),f_2(\omega)), & \omega \in \Omega_{diff}(f_1)\cap\Omega_{diff}(f_2); \\ \rho_{spec}(f_1(\omega),f_2(\omega)), & \omega \in \Omega_{spec}(f_1)\cap\Omega_{spec}(f_2)\cap \\ & \{\omega \,|\, \rho_{spec}(f_1,f_2)(\omega) < \Delta_2\}; \\ \Delta_3, & \omega \in \Omega_{spec}(f_1)\cap\Omega_{spec}(f_2)\cap \\ & \{\omega \,|\, \rho_{spec}(f_1,f_2)(\omega) \geq \Delta_2\}; \\ \Delta_4, & \omega \in (\Omega_{spec}(f_1)\cap\Omega_{diff}(f_2)) \\ & \cup(\Omega_{diff}(f_1)\cap\Omega_{spec}(f_2))\,. \end{cases} \tag{19}$$

Here Δ_1, Δ_2 Δ_3 and Δ_4 are constants, with Δ_3 smoothing out the influence of large peaks and of gross errors in measurements of peaks, and with Δ_4 penalizing missing or added peaks. Δ_1 determines the level where we switch the regime in our analysis of diffuse and specular components, while Δ_2 quantifies the notion of large peaks and measurements with potentially gross errors.

Definition 4. *We define the* metric (distance) μ_{BRDF} *on $\mathcal{F}_4$ as follows. For any BRDFs f_1, $f_2 \in \mathcal{F}_4$, set*

$$\mu_{BRDF}(f_1,f_2) = \int_\Omega \rho_{BRDF}(f_1,f_2)(\omega)\, d\mu_\Omega(\omega)\,. \tag{20}$$

An important example is given by L_p-norms. If $\mu_{diff} = L_p^p$, then $\rho_{diff}(x,y) = |x-y|^p$. As μ_{diff} we can reasonably use any L_p-based measure. It is possible to use an L_{p_1}-based measure μ_{spec}, possibly for some $p_1 \neq p$. A number of truncated measures has been considered in robust statistics.

A proper choice of parameters $\Delta_1,\ldots,\Delta_4$ is closely related to the model selection problem, see [Langovoy 2007].

The above expression for μ_{BRDF} can be computed explicitly in special cases, for example, when both BRDFs are known explicitly beforehand, either analytically or in a parametric form. This will not be the case when at least one of these BRDFs belongs to a real material, as in this case we would only have a finite set of measurements of $\rho_{BRDF}(f_1,f_2)(\omega)$ in our disposal. To account for applications to real data, we introduce the following approximate empirical quasi-distance between BRDFs.

Definition 5. *Suppose that BRDFs f_1 and f_2 were measured on the following collection of points:*

$$\Omega_{meas} = \left\{ \left(\theta_i^{(p)},\varphi_i^{(p)},\theta_r^{(q)},\varphi_r^{(q)}\right) \,\middle|\, \left(\theta_i^{(p)},\varphi_i^{(p)}\right) \in \Omega_{inc}\,,\ \left(\theta_r^{(q)},\varphi_r^{(q)}\right) \in \Omega_{refl}(p) \right\}. \tag{21}$$

We define the empirical metric (distance) $\widehat{\mu}_{BRDF}$ *on $\mathcal{F}_4$ as follows. For any BRDFs f_1, $f_2 \in \mathcal{F}_4$, that are both measured on Ω_{meas}, set*

$$\widehat{\mu}_{BRDF}(f_1,f_2) = \frac{\mu_\Omega(\Omega)}{\left|\Omega_{meas}\right|} \sum_{\omega\in\Omega_{meas}} \rho_{BRDF}(f_1,f_2)(\omega)\,. \tag{22}$$

In other words, according to Lemma 1 below,

$$\widehat{\mu}_{BRDF}(f_1,f_2) = \frac{\pi^2}{8\left|\Omega_{meas}\right|} \sum_{\omega\in\Omega_{meas}} \rho_{BRDF}(f_1,f_2)(\omega)\,. \tag{23}$$

Under proper smoothness conditions on both BRDFs and on the sampling points, $\widehat{\mu}_{BRDF}$ as a Riemann sum asymptotically approximates the Lebesgue integral equal to μ_{BRDF}. In this case, μ_{BRDF} is the asymptotic

limit of $\widehat{\mu}_{BRDF}$. However, in practice the size of the set Ω_{meas}, and especially the size of Ω_{inc}, can be small and the situation can be far from the asymptotic regime. For this reason, we do not aim to approximate μ_{BRDF} by $\widehat{\mu}_{BRDF}$ in our applications.

We now propose a useful simplification of the above quasi-distance. We noticed that, for actual BRDF measurements, it is often reasonable to pick $\Delta_1 \approx 1$. Moreover, often $\rho_{diff}(x,y) = |x-y|^p$ is used as the element of distance. Therefore, it often makes sense in practice to choose $\Delta_1 = \Delta_2$. For similar reasons, $\Delta_3 = \Delta_4$ can be a reasonable choice in many applications. Therefore, the following simplification of Definition 3 is often useful.

Definition 6. *Let f_1, f_2 be BRDFs. Define the* element of distance *between f_1 and f_2 in $\mathcal{F}_4$ at a point ω as*

$$\rho_{BRDF}(f_1,f_2)(\omega) = \begin{cases} \rho_{diff}(f_1(\omega),f_2(\omega)), & \omega \in \Omega_{diff}(f_1)\cap\Omega_{diff}(f_2); \\ \rho_{spec}(f_1(\omega),f_2(\omega)), & \omega \in \Omega_{spec}(f_1)\cap\Omega_{spec}(f_2)\cap \\ & \{\omega \,|\, \rho_{spec}(f_1,f_2)(\omega) < \Delta_1\}; \\ \Delta_2, & \omega \in \Omega_{spec}(f_1)\cap\Omega_{spec}(f_2)\cap \\ & \{\omega \,|\, \rho_{spec}(f_1,f_2)(\omega) \geq \Delta_1\}; \\ \Delta_2, & \omega \in (\Omega_{spec}(f_1)\cap\Omega_{diff}(f_2)) \\ & \cup(\Omega_{diff}(f_1)\cap\Omega_{spec}(f_2))\,. \end{cases} \tag{24}$$

Here Δ_1 and Δ_2 are pre-selected constants, with Δ_2 penalizing missing or added peaks and smoothing out the influence of large peaks and of gross errors in measurements of peaks. Δ_1 determines the level where we switch the regime in our analysis.

Definitions 2 and 4 apply in this case without changes. To simplify the presentation, to the end of this paper we work with the simplified quasi-distance.

The following two continuations of Examples 1 and 2 illustrate how these definitions provide a physically sensible quasi-metric.

Example 1 (continuation). Suppose ρ_{diff} and ρ_{spec} are L_p-based, then it makes sense to compare the induced quasi-metric μ_{BRDF} with L_p^p. These illuminated balls look very similar to a human observer, but an L_p-distance between the BRDFs f_1 and f_2 is large. In order to call our quasi-metric physically sensible, it is desirable for μ_{BRDF} to reflect the fact that these balls look very similar. And, indeed, if Δ_1 is smaller than the difference between the heights of two peaks and if Δ_1 is such that both peaks are correctly singled out as peaks, and if Δ_2 is not too big so that it actually penalizes the large difference between the peaks by any amount, then

$$\mu_{BRDF}(f_1,f_2) < L_p^p(f_1,f_2)\,.$$

This means that μ_{BRDF} reflects the similarity between these two illuminated balls better than the L_p-distance.

Example 2 (continuation). Once again, suppose ρ_{diff} and ρ_{spec} are L_p-based and compare the μ_{BRDF} with L_p^p. Here an L_p-distance is small, since a very thin second peak of f_2 gives a small contribution to the integral, but the difference between the balls is substantial for a human observer. A good distance on $\mathcal{F}_4$ should reflect the fact that these balls look very different. In this example, if Δ_1 is such that it separates the thin second peak of f_2 from the diffuse part of f_2, and if Δ_2 is big enough so that it actually penalizes the extra peak of f_2 by any amount, then

$$\mu_{BRDF}(f_1, f_2) > L_p^p(f_1, f_2)\,.$$

This means that μ_{BRDF} reflects the dissimilarity between these two illuminated balls better than the L_p-distance.

8. BASIC PROPERTIES OF NEW DISTANCES ON THE SPACE OF BRDFS

Proposition 1. *Assuming that for any $f \in \mathcal{F}_4$, the sets $\Omega_{spec}(f)$ and $\Omega_{diff}(f)$ are measurable, we have the following equivalent representation (decomposition):*

$$\mu_{BRDF}(f_1, f_2) = \mu_{diff}(f_1, f_2)\Big|_{\Omega_{diff}(f_1)\cap\Omega_{diff}(f_2)} + \tag{25}$$

$$\mu_{spec}(f_1, f_2)\Big|_{\Omega_{spec}(f_1)\cap\Omega_{spec}(f_2)\cap\{\omega\,|\,\rho_{spec}(f_1,f_2)(\omega)<\Delta_1\}} + \tag{26}$$

$$\Delta_2 \cdot \mu_\Omega\Big(\Omega_{spec}(f_1)\cap\Omega_{spec}(f_2)\cap\{\omega\,|\,\rho_{spec}(f_1,f_2)(\omega) \geq \Delta_1\}\Big) \tag{27}$$

$$\Delta_2 \cdot \mu_\Omega\Big(\big(\Omega_{spec}(f_1)\cap\Omega_{diff}(f_2)\big)\cup\big(\Omega_{diff}(f_1)\cap\Omega_{spec}(f_2)\big)\Big)\,. \tag{28}$$

Proof. Follows directly from (24) and (20). □

Lemma 1. *Let μ_Ω be the Lebesgue measure (i.e., the Euclidean volume) on the set $\Omega \subset \mathbb{R}^4$, and let Ω be defined by (9). Then*

$$\mu_\Omega(\Omega) = \frac{\pi^2}{8}\,. \tag{29}$$

Proof. $\mu_\Omega(\Omega) = \mu_\Omega(S^3)$, where S^3 is 1/8 of a 3-sphere in $\mathbb{R}^4$. For the octant S^3,

$$\mu_\Omega(S^3) = \frac{\pi^2}{4}\cdot\frac{1}{\Gamma(4/2)} = \frac{\pi^2}{8}\,.$$

□

Proposition 2. *Under the above assumptions, both sets in (27) and (28) are μ_Ω-measurable, and*

$$\mu_\Omega\Big(\Omega_{spec}(f_1)\cap\Omega_{spec}(f_2)\cap\{\omega\,|\,\rho_{spec}(f_1,f_2)(\omega) \geq \Delta_1\}\Big) < +\infty\,,$$

$$\mu_\Omega\Big(\big(\Omega_{spec}(f_1)\cap\Omega_{diff}(f_2)\big)\cup\big(\Omega_{diff}(f_1)\cap\Omega_{spec}(f_2)\big)\Big) < +\infty\,.$$

Proof. Follows directly from Lemma 1. □

Note that calling μ_{BRDF} a measure or a distance is an abuse of terminology, since μ_{BRDF} does not always satisfy the axioms for distances. It would be more appropriate to call μ_{BRDF} either quasi- or pseudo-distance. A similar situation is true for the Kullback-Leibler information measure (or information distance) [Kullback and Leibler 1951]. This is not actually a distance, but its other properties make the information distance one of the most popular distance measures used in statistical model selection or in machine learning.

9. AN ABSOLUTE SCALE OF DISTANCES ON THE SPACE OF BRDFS

A very useful property of μ_{BRDF} is that it is uniformly bounded from above, namely, $\mu_{BRDF}(f_1, f_2) \leq \mu_{MAX} < +\infty$ for any pair of BRDFs f_1 and f_2. In the case that the bounding constant μ_{MAX} is known, either exactly or approximately, we receive an absolute scale (from 0 to μ_{MAX}) for evaluating the closeness of BRDFs to each other. For example, a value of $\mu_{BRDF}(f_1, f_2)$ close to μ_{MAX} indicates that f_1 and f_2 are extremely far apart. Usual L_p-distances do not possess this useful property. The rest of this section is devoted to establishing useful explicit bounds on μ_{BRDF}.

From now on, we assume that, for any $0 < \Delta < +\infty$, the function

$$M_{diff}(\Delta) = \sup_{(x,y)\in[0,\Delta]\times[0,\Delta]} \rho_{diff}(x, y) \tag{30}$$

is well defined. For example, if $\mu_{diff} = L_p^p$, then $\rho_{diff}(x, y) = |x - y|^p$, and $M_{diff}(\Delta) = \Delta^p$.

Proposition 3. *Under the above assumptions, $\mu_{BRDF}(f_1, f_2) \leq \mu_{MAX} < +\infty$ for any pair of BRDFs f_1 and f_2. Moreover,*

$$\mu_{BRDF}(f_1, f_2) \leq \frac{\pi^2}{8}\big(\Delta_1 + 2\Delta_2 + M_{diff}(\Delta_1)\big)\,. \tag{31}$$

Proof. Follows via crude estimates from Lemma 1 and proposition 1.

While the estimate (31) establishes and quantifies our idea of boundedness of the new quasi-distance, this bound is still not very useful for establishing a good absolute scale for BRDF closeness. This bound is too crude. We propose more useful and much tighter bounds in the following theorem.

Theorem 1. *Under the above assumptions, $\mu_{BRDF}(f_1, f_2) \leq \mu_{MAX} < +\infty$ for any pair of BRDFs f_1 and f_2. More precisely,*

$$\mu_{BRDF}(f_1, f_2) \leq \frac{\pi^2}{8}\big(\Delta_1 + \Delta_2\big) + \mu_\Omega\big(\Omega_{diff}(f_1) \cap \Omega_{diff}(f_2)\big)\big(M_{diff}(\Delta_1) - \Delta_1\big)\,. \tag{32}$$

As an absolute bound, we have

$$\mu_{BRDF}(f_1, f_2) \leq \frac{\pi^2}{8}\big(\Delta_2 + M_{diff}(\Delta_1)\big)\,. \tag{33}$$

Proof.

$$\mu_{diff}(f_1, f_2)\Big|_{\Omega_{diff}(f_1)\cap\Omega_{diff}(f_2)} = \int_{\Omega_{diff}(f_1)\cap\Omega_{diff}(f_2)} \rho_{diff}(f_1(\omega), f_2(\omega))\, d\mu_\Omega(\omega)$$

$$\leq \mu_\Omega\Big(\Omega_{diff}(f_1) \cap \Omega_{diff}(f_2)\Big) \cdot \sup_{\omega\in\Omega_{diff}(f_1)\cap\Omega_{diff}(f_2)} \Big(\rho_{diff}(f_1(\omega), f_2(\omega))\Big)\,. \tag{34}$$

Taking into account the definition of $\Omega_{diff}(f_i)$ in Definition 2, we obtain that

$$\sup_{\omega\in\Omega_{diff}(f_1)\cap\Omega_{diff}(f_2)} \Big(\rho_{diff}(f_1(\omega), f_2(\omega))\Big) \leq \sup_{(x,y)\in[0,\Delta_1]\times[0,\Delta_1]} \Big(\rho_{diff}(x, y)\Big)\,. \tag{35}$$

Now (35) together with (34) and (30) leads to

$$\mu_{diff}(f_1,f_2)\Big|_{\Omega_{diff}(f_1)\cap\Omega_{diff}(f_2)} \le \mu_\Omega\Big(\Omega_{diff}(f_1)\cap\Omega_{diff}(f_2)\Big)\cdot \sup_{(x,y)\in[0,\Delta_1]\times[0,\Delta_1]}\Big(\rho_{diff}(x,y)\Big) \le \mu_\Omega\Big(\Omega_{diff}(f_1)\cap\Omega_{diff}(f_2)\Big)\cdot M_{diff}(\Delta_1)\,. \tag{36}$$

Notice that, in view of the decomposition in Definition 2,

$$\mu_\Omega\Big(\Omega_{diff}(f_1)\cap\Omega_{diff}(f_2)\Big)+ \mu_\Omega\Big(\Omega_{spec}(f_1)\cap\Omega_{spec}(f_2)\cap\{\omega\,|\,\rho_{spec}(f_1,f_2)(\omega)<\Delta_1\}\Big)\le\mu_\Omega(\Omega)\,, \tag{37}$$

and

$$\mu_\Omega\Big(\Omega_{spec}(f_1)\cap\Omega_{spec}(f_2)\cap\{\omega\,|\,\rho_{spec}(f_1,f_2)(\omega)\ge\Delta_1\}\Big)+ \mu_\Omega\Big(\big(\Omega_{spec}(f_1)\cap\Omega_{diff}(f_2)\big)\cup\big(\Omega_{diff}(f_1)\cap\Omega_{spec}(f_2)\big)\Big)\le\mu_\Omega(\Omega)\,. \tag{38}$$

Applying (37), we deduce

$$\mu_{spec}(f_1,f_2)\Big|_{\Omega_{spec}(f_1)\cap\Omega_{spec}(f_2)\cap\{\omega\,|\,\rho_{spec}(f_1,f_2)(\omega)<\Delta_1\}} = \int_{\Omega_{spec}(f_1)\cap\Omega_{spec}(f_2)\cap\{\omega\,|\,\rho_{spec}(f_1,f_2)(\omega)<\Delta_1\}}\rho_{spec}(f_1(\omega),f_2(\omega))\,d\mu_\Omega(\omega)$$

$$\le \mu_\Omega\Big(\Omega_{spec}(f_1)\cap\Omega_{spec}(f_2)\cap\{\omega\,|\,\rho_{spec}(f_1,f_2)(\omega)<\Delta_1\}\Big) \times\sup_{\omega\in\Omega_{spec}(f_1)\cap\Omega_{spec}(f_2)\cap\{\omega\,|\,\rho_{spec}(f_1,f_2)(\omega)<\Delta_1\}}\Big(\rho_{spec}(f_1(\omega),f_2(\omega))\Big)$$

$$\le \sup_{\omega\in\Omega_{spec}(f_1)\cap\Omega_{spec}(f_2)\cap\{\omega\,|\,\rho_{spec}(f_1,f_2)(\omega)<\Delta_1\}}\Big(\rho_{spec}(f_1(\omega),f_2(\omega))\Big) \times\Big(\mu_\Omega(\Omega)-\mu_\Omega\Big(\Omega_{diff}(f_1)\cap\Omega_{diff}(f_2)\Big)\Big)$$

$$\le \Delta_1\cdot\Big(\mu_\Omega(\Omega)-\mu_\Omega\Big(\Omega_{diff}(f_1)\cap\Omega_{diff}(f_2)\Big)\Big) = \frac{\pi^2}{8}\,\Delta_1-\mu_\Omega\Big(\Omega_{diff}(f_1)\cap\Omega_{diff}(f_2)\Big)\,\Delta_1\,. \tag{39}$$

Applying (38), we deduce

$$\begin{aligned}
&\Delta_2 \cdot \mu_\Omega\Big(\Omega_{spec}(f_1) \cap \Omega_{spec}(f_2) \cap \{\omega \,|\, \rho_{spec}(f_1, f_2)(\omega) \geq \Delta_1\}\Big) \\
&+ \Delta_2 \cdot \mu_\Omega\Big(\big(\Omega_{spec}(f_1) \cap \Omega_{diff}(f_2)\big) \cup \big(\Omega_{diff}(f_1) \cap \Omega_{spec}(f_2)\big)\Big) \quad \leq \\
&\Delta_2 \cdot \mu_\Omega\Big(\Omega_{spec}(f_1) \cap \Omega_{spec}(f_2) \cap \{\omega \,|\, \rho_{spec}(f_1, f_2)(\omega) \geq \Delta_1\}\Big) \\
+ \Delta_2 \Big(\mu_\Omega(\Omega) - \mu_\Omega\Big(&\Omega_{spec}(f_1) \cap \Omega_{spec}(f_2) \cap \{\omega \,|\, \rho_{spec}(f_1, f_2)(\omega) \geq \Delta_1\}\Big)\Big) \quad = \\
&= \Delta_2 \, \mu_\Omega(\Omega) = \frac{\pi^2}{8} \, \Delta_2 \,. \qquad (40)
\end{aligned}$$

Substituting (36), (39) and (40) into the decomposition of Proposition 1 and summing up the terms, we prove (32).

After substituting Lemma 1 and (37) into (32), simple arithmetics leads to (33).

Notice that (33) (and even more so (32)) is a much better bound than the standard one given in Proposition 3.

10. CONCLUSIONS

The BRDF is one of the fundamental concepts in such diverse fields as multidimensional reflectometry, computer graphics and computer vision. In this paper, we treated BRDF measurements as samples of points from high-dimensional non-linear non-convex manifold. We have shown that statistical analysis of BRDF measurements has to account both for the nonlinear structure of the data as well as for ill-behaved noise. Standard statistical methods can not be safely directly applied to BRDF data. We clarified certain pitfalls in the analysis of BRDF data.

We proposed a new class of measures of quality of fit for BRDF models. We will use these measures to evaluate the influence of measurement and model errors on both real and simulated BRDFs. Our measure of distance between BRDFs is leading to physically meaningful conclusions for basic applications of BRDF data analysis. This is a useful property as our analysis has to be applicable to physical objects and real data.

We studied basic properties of new quasi-distances on the space of BRDFs, proved the boundedness of these quasi-measures, and thus shown that they induce an absolute scale of distances on the space of BRDFs. Our bounds are much stronger than the inequalities obtained by standard methods, and therefore we provide better approximations of induced absolute scales of distances on the space of BRDFs.

REFERENCES

Arvo, J., Torrance, K., and Smits, B. 1994. A framework for the analysis of error in global illumination algorithms. In *Proceedings of the 21st annual conference on Computer graphics and interactive techniques*. ACM, 75–84.

Ashikhmin, M. and Premoze, S. 2007. Distribution-based brdfs. *Unpublished Technical Report, University of Utah 2*.

Ashikhmin, M. and Shirley, P. 2000. An anisotropic phong brdf model. *Journal of graphics tools 5,* 2, 25–32.

Blinn, J. F. 1977. Models of light reflection for computer synthesized pictures. In *Proceedings of the 4th annual conference on Computer graphics and interactive techniques*. SIGGRAPH '77. ACM, New York, NY, USA, 192–198.

Cook, R. L. and Torrance, K. E. 1981. A reflectance model for computer graphics. In *ACM Siggraph Computer Graphics*. Vol. 15. ACM, 307–316.

Fairbairn, M. B. 2005. Planetary Photometry: The Lommel-Seeliger Law. *Journal Royal Astronomical Society Canada 99*, 92.

Fleming, R. W., Dror, R. O., and Adelson, E. H. 2003. Real-world illumination and the perception of surface reflectance properties. *Journal of Vision 3,* 5, 3.

He, X. D., Torrance, K. E., Sillion, F. X., and Greenberg, D. P. 1991. A comprehensive physical model for light reflection. In *ACM SIGGRAPH Computer Graphics*. Vol. 25. ACM, 175–186.

Höpe, A. and Hauer, K.-O. 2010. Three-dimensional appearance characterization of diffuse standard reflection materials. *Metrologia 47,* 3, 295.

Höpe, A., Koo, A., Forthmann, C., Verdu, F., Manoocheri, F., Leloup, F., Obein, G., Wübbeler, G., Ged, G., Campos, J., et al. 2014. xd-reflect-" multidimensional reflectometry for industry" a research project of the european metrology research program (emrp). In *12th International Conference on New Developments and Applications in Optical Radiometry (NEWRAD 2014)*.

Kullback, S. and Leibler, R. A. 1951. On information and sufficiency. *The Annals of Mathematical Statistics*, 79–86.

Lafortune, E. P., Foo, S.-C., Torrance, K. E., and Greenberg, D. P. 1997. Non-linear approximation of reflectance functions. In *Proceedings of the 24th annual conference on Computer graphics and interactive techniques*. ACM Press/Addison-Wesley Publishing Co., 117–126.

Lambert, J. and Anding, E. 1892. *Lamberts Photometrie: (Photometria, sive De mensura et gradibus luminis, colorum et umbrae) (1760)*. Number v. 1-2 in Ostwalds Klassiker der exakten Wissenschaften. W. Engelmann.

Langovaya, A., Kuhnt, S., and Chouikha, H. 2013. Correspondence analysis in the case of outliers. In *Classification and Data Mining*. Springer, 63–70.

Langovoy, M. 2007. *Data-driven goodness-of-fit tests*. University of Göttingen, Göttingen. Ph.D. thesis.

Langovoy, M., Habeck, M., and Schoelkopf, B. 2011a. Adaptive nonparametric detection in cryo-electron microscopy. In *Proceedings of the 58-th World Statistical Congress*. Session: High Dimensional Data. 4456 – 4461.

Langovoy, M., Habeck, M., and Schoelkopf, B. 2011b. Spatial statistics, image analysis and percolation theory. In *The Joint Statistical Meetings Proceedings*. Time Series and Network Section. American Statistical Association, Alexandria, VA, 5571 – 5581.

Langovoy, M. and Shneer, V. 2014. Perfect simulation of heavy-tailed distributions and extreme events. *In preparation*.

Langovoy, M., Wübbeler, G., and Elster, C. 2014. Statistical analysis of BRDF data for computer graphics and metrology. *To appear in the Proceedings of The World Congress on Engineering and Computer Science*.

Mahalanobis, P. C. 1936. On the generalized distance in statistics. *Proceedings of the National Institute of Sciences (Calcutta) 2*, 49–55.

Matusik, W. 2003. A data-driven reflectance model. Ph.D. thesis, Citeseer.

Matusik, W., Pfister, H., Brand, M., and McMillan, L. 2003. A data-driven reflectance model. In *ACM Transactions on Graphics (TOG)*. Vol. 22. ACM, 759–769.

Ngan, A., Durand, F., and Matusik, W. 2005. Experimental analysis of brdf models. In *Proceedings of the Sixteenth Eurographics conference on Rendering Techniques*. Eurographics Association, 117–126.

Nicodemus, F. E. 1965. Directional reflectance and emissivity of an opaque surface. *Applied Optics 4*, 767 – 775.

Obein, G., Ouarets, S., and Ged, G. 2014. Evaluation of the shape of the specular peak for high glossy surfaces. In *IS&T/SPIE Electronic Imaging*. International Society for Optics and Photonics, 901805–901805.

Oren, M. and Nayar, S. K. 1995. Generalization of the lambertian model and implications for machine vision. *International Journal of Computer Vision 14,* 3, 227–251.

Ouarets, S., Leroux, T., Rougie, B., Razet, A., and Obein, G. 2013. A high resolution set up devoted to the measurement of the bidirectional reflectance distribution function around the specular peak, at lne-cnam. In *16th International Congress of Metrology*. EDP Sciences, 14008.

Phong, B. T. 1975. Illumination for computer generated pictures. *Commun. ACM 18,* 6, 311–317.

Rushmeier, H., Ward, G., Piatko, C., Sanders, P., and Rust, B. 1995. Comparing real and synthetic images: Some ideas about metrics. In *Rendering Techniques 95*. Springer, 82–91.

Shirley, P., Smits, B., Hu, H., and Lafortune, E. 1997. A practitioners' assessment of light reflection models. In *Computer Graphics and Applications, 1997. Proceedings., The Fifth Pacific Conference on*. IEEE, 40–49.

Simonot, L. 2009. Photometric model of diffuse surfaces described as a distribution of interfaced lambertian facets. *Appl. Opt. 48,* 30, 5793–5801.

Sobolev, S. On a theorem of functional analysis.

Torrance, K. E. and Sparrow, E. M. 1967. Theory for off-specular reflection from roughened surfaces. *JOSA 57,* 9, 1105–1112.

Ward, G. J. 1992. Measuring and modeling anisotropic reflection. In *ACM SIGGRAPH Computer Graphics*. Vol. 26. ACM, 265–272.